Energy Conversion and Management 167 (2018) 125–133

Contents lists available at ScienceDirect

Energy Conversion and Management

journal homepage: www.elsevier.com/locate/enconman

Exergy efficiency of solar energy conversion to biomass of green macroalgae Ulva (Chlorophyta) in the photobioreactor

Meiron Zollmann[a], Hadar Traugott[b], Alexander Chemodanov[a], Alexander Liberzon[b], Alexander Golberg[a,*]

[a] Porter School of Environmental Studies, Tel Aviv University, Israel
[b] School of Mechanical Engineering, Tel Aviv University, Israel

ARTICLE INFO

Keywords:
Macroalgae
Energy conversion efficiency
Exergy
Photobioreactor
Seagriculture

ABSTRACT

Offshore production of macroalgae biomass, which was recently given the name seagriculture, is one of the important but least explored alternative energy resources. Unlike microalgae, macroalgae cultivation can be done offshore and therefore brings real news to the biofuel – food land agriculture conflict. A wide variety of small-scale laboratory experiments are done lately in order to deepen the knowledge and develop expertise in macroalgae cultivation and its downstream processing. For energy applications, it is common to evaluate the performance of an energy source or system in exergy efficiency terms. Another important parameter that is evaluated to determine the system's environmental impact is it's volumetric and areal footprint. The current work examines two exergy efficiency indexes, the Exergy Efficiency (EE), which takes into account all exergy inputs, and the Exergy Return On Investment (ExROI), that includes only fossil fuel exergy inputs, both on a green macroalgae Ulva grown in the macroalgae photobioreactor system (MPBR) incorporated into a building. Cultivation of macroalgae in the building embedded MPBR achieved maximal values of 0.012 and 0.22 for EE and ExROI, compared to a range of 0.05–8.34 and 0.013–0.327 found in published papers of microalgae systems. In addition, a modelled optimization of the initial biomass density leads to maximal values of about 0.035 for EE and 0.433 for ExROI, while further improvement may be achieved by optimization of nutrient addition and mixing methodology. This work demonstrates a tool to measure the performance of laboratory scale macroalgae biomass cultivation systems, followed by preliminary efficiency and environmental impact values, important for future upscaling.

1. Introduction

Rapidly growing energy consumption and consequential environmental effects have lead in recent years to a global realization of the urgent need to develop alternative renewable energy sources [1–3]. Offshore production of macroalgae biomass [4,5], which was recently given the name seagriculture [6], is one of the important but least explored alternative energy resources. Macroalgae produced in offshore farms is a potential feedstock for marine biorefineries, designed to process the biomass into fuel, food, chemicals and high-value products [7,8]. Therefore, this alternative offers also new capabilities to cope with the water-energy-land-food nexus [3,9].

Macroalgae relate to multicellular aquatic species from three groups: red, brown and green algae [10]. Till the 1950s macroalgae were mostly wild-harvested. Today, after the domestication of some species, macroalgae are cultivated globally, but still mostly in the Asian-Pacific region, where cultivation originated [11]. Most widely spread macroalgae cultivation industries include the edible red algae such as Japanise Nori (Pyropia), and the brown Kelp Wakame (*Undaria pinnatifida*) and Kombu (*Saccharina japonica*). A large demand exists also for the red algae hydrocolloids, carrageenan, which can be extracted from *Eucheuma* sp. and *Kappaphycus* sp., and agar, which can be extracted from agarophytes such as *Gelidium*, *Gracilaria*, *Pterocladia,* and *Gelidiella*. The success of these industries can be attributed to a combination of basic science and consumer demand [11].

Green macroalgae, although produced also as a food product, attract most research attention due to the nutrient uptake and fast-growing abilities of some species, such as the *Ulva* sp. The first enables utilizing *Ulva* for biofiltration of fishponds effluents [12,13]. The second, combined with high carbohydrate contents, places the *Ulva* sp. as a leading alternative for biorefinery and bioenergy feedstock [14,15]. Numerous studies have examined the different possibilities of extracting energy

* Corresponding author.
E-mail address: agolberg@tauex.tau.ac.il (A. Golberg).

https://doi.org/10.1016/j.enconman.2018.04.090
Received 22 January 2018; Received in revised form 21 April 2018; Accepted 23 April 2018
0196-8904/

from *Ulva* and producing fuels in the form of biogas, bioethanol, biobutanol, and others [5,16–18]. However, energy stock seagriculture is still undeveloped. Increasing attention and research in this field requires suitable tools to evaluate the performance of macroalgae cultivation systems.

Energy and exergy analysis are common methodologies used to evaluate the performance of energy harvesting systems [1,19] and an often-applied impact category in life cycle assessments (LCA) [20–23]. Traditional fossil fuels such as coal, oil, and gas, although regarded as polluting and unsustainable, are still highly available and consist of high energetic densities and thus have a clear exergy and economic advantage in the short term. Alternative energy sources, before being applied in large scales, need to prove positive exergy efficiencies and an economic feasibility [24]. Energy conversion efficiencies are represented in different works by different indicators. Therefore, the applied indicators and scope of the analysis must be clearly defined and rationalized, including exact descriptions of calculation procedures [20].

Two important dimensionless performance efficiency indicators in the biofuel field are the Exergy Efficiency (EE) [25] and the Exergy Return On Investment (ExROI) [26– 32]. In the current work, EE considers all exergy inputs and outputs and is supposed to reflect the thermodynamic balance, accounting for the irreversibility of the conversion processes. The ExROI calculation excludes exergy inputs that do not derive from fossil fuels and thus is more useful for environmental impact evaluations. These definitions are presented mathematically in Eqs. (1) and (2), based on [33]. These equations are somewhat general, and thus the exact components of both parameters must be defined in each system according to its specific characteristics [20,33–37].

$$EE = \frac{\text{Total exergy output}}{\text{Total exergy input}} \tag{1}$$

$$ExROI = \frac{\text{Total exergy output}}{\text{Total fossil exergy input}} \tag{2}$$

Macroalgae photobioreactors (MPBR) [6], medium scale laboratory cultivation systems, can allow semi-open environments, thus enabling improved simulations of field conditions towards necessary future upscale. MPBRs were developed only recently, following the microalgae cultivation in photobioreactors (PBR) that has been performed for about a decade [38]. Consequently, no exergy efficiency values were yet published for MPBR systems. However, previous works have estimated exergetic performances of microalgae systems of different kinds, from the industrialized raceway ponds and tubular or flat-plate PBRs, to the building integrated façade PBRs [34–37,39–43]. These estimations usually focused on the input streams of energy consumed for mixing and thermal regulation of the system and on the energy content of the produced biomass as an output stream, ignoring other energy requirements for the construction of the system or for the processing of the biomass [34–36].

The current work suggests EE and ExROI formulas for the evaluation of these indicators for a closed MPBR system. This kind of energy budget analysis cannot be done in an offshore, uncontrolled, system. Furthermore, this work evaluates first MPBR exergetic efficiency values and compares them to other biomass production systems. In addition, occupational areal and volumetric productivity are evaluated and compared as an additional important evaluation parameter. Finally, a sensitivity analysis is performed, pointing out requested future system optimization steps for large-scale production on and off-shore.

2. MPBR exergetic efficiency models

The suggested models implement the EE and ExROI indicators on a closed MPBR, focusing on the main process exergy inputs and outputs. The MPBR EE includes direct exergy inputs in the form of solar energy (E_{sol}) and electrical energy (E_{elec}) and indirect exergy inputs, in the form of nutrients (E_{nut}) and biomass ($E_{bio\ initial}$). This part can also be called cumulative exergy demand [20]. It should be mentioned that the inclusion of solar energy input is not common in other exergy balance analysis, and may be of importance in intensive cultivations where irradiance can be controlled and manipulated [44–46]. The only relevant output parameter for the efficiency calculation is the produced biomass ($E_{produced\ bio}$), which is the accumulated biomass. Input and output exergy streams are illustrated in Fig. 1. Other exergy streams, related to labor, capital, waste and ecosystem services [47] are not taken into account as for the small scale of these systems. The second indicator, the ExROI, excludes from the calculation the exergy inputs that do not derive from fossil fuels, such as solar irradiance and biomass. EE is described in Eq. (3), and ExROI is described in Eq. (4). Mathematical representation and detailed calculation of each component are described in the methods chapter.

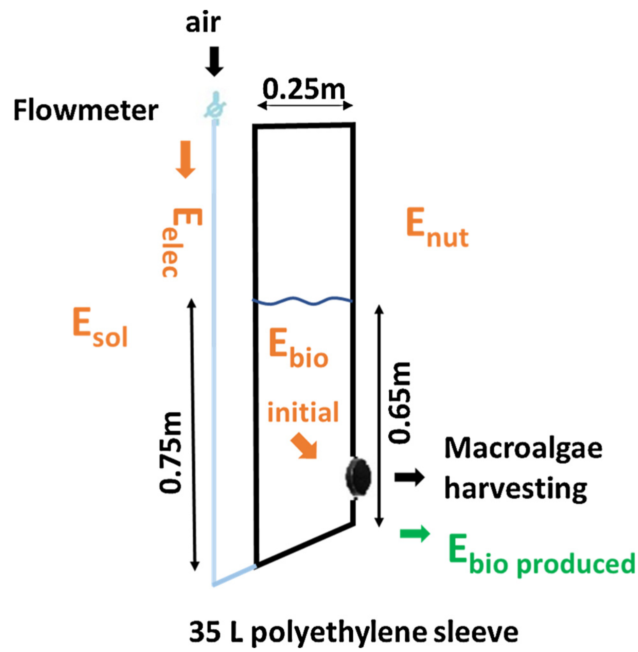

Fig. 1. System exergy input and output streams illustration. Input streams: solar energy (E_{sol}), electrical energy (E_{elec}) and energy embedded in initial biomass ($E_{bio\ initial}$) and in nutrients (E_{nut}). Output stream: energy embedded in produced biomass ($E_{bio\ produced}$).

$$EE = \frac{E_{produced\ bio}}{E_{sol} + E_{elec} + E_{nut} + E_{initial\ bio}} \tag{3}$$

$$ExROI = \frac{E_{produced\ bio}}{E_{elec} + E_{nut}} \tag{4}$$

3. Materials and methods

3.1. Marine macroalgae biomass

Green leafy macroalgae *Ulva* sp. (Fig. 2a) was collected from Haifa during spring 2016 and cultivated in a closed macroalgae photobioreactor system (MPBR) built for research purposes in the University of Tel Aviv [6] (Fig. 2b). During cultivation, nutrient concentrations in seawater were maintained at 6.4 mg l^{-1} of nitrogen and 0.97 mg l^{-1} of phosphorus by fertilizing with ammonium nitrate (NH_4NO_3, Haifa Chemicals Ltd, IS) and phosphoric acid (H_3PO_4, Haifa Chemicals Ltd, IS). CO_2 was supplied by bubbling air. A full description of this MPBR can be found in [6].

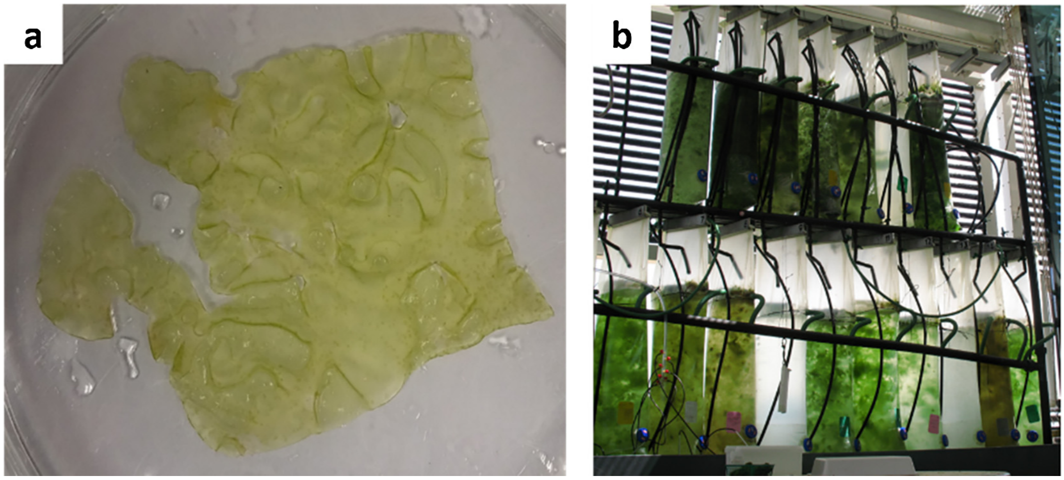

Fig. 2. Illustration of: (a) *Ulva* thallus and (b) MPBR system [6], used in this study.

3.2. Experimental setup

A closed vertical polyethylene photobioreactor was used. This photobioreactor includes one reactor welded from 200 µm thick polyethylene sleeve (Polytiv, Israel, Length 1 m, Width 0.4 m) with embedded anti-UV protection. The reactor was filled up with 35 L of artificial seawater (ASW, 38–40 ppt, 7.9–8.2 pH) composed of 35 L of distilled water (Zalion Ltd, IS), and 1433.25 g sea salt (Red Sea Ltd). Air bubble mixing was provided from the bottom at a rate of 2 L min^{-1}. Fresh weight (FW) of the biomass was determined using an analytical scale (Mettler Toledo, PB-S model, Switzerland, 0.01 g precision) after removing surface water using an electric centrifuge (Spin Dryer, CE-88, Beswin).

First, 200 g FW of Ulva from the MPBR was weighed and cultivated for 6–8 days of acclimation in the reactor, filled up with 35-liter ASW without added nutrients. Acclimation was done to minimize effects of environmental changes and of nutritional history on growth rates [48]. Next, 10 g FW was weighed and cultivated for 3 weeks in a similar reactor, filled up with new ASW. The cultivated algae were fertilized with concentrations of 6.02 mg l^{-1} of nitrogen ($NaNO_3$, Merck, Germany) and 0.832 mg l^{-1} of phosphorus (NaH_2PO_4, CalBiochem, CA) once a week, in a molar ratio of 16:1 N:P, to prevent P limitation [48]. These concentrations were supposed to ensure excess nutrients along the whole study [49–51]. The fertilization was done using a premade stock solution, filtered through 0.22-µm disposable filters and kept in refrigeration. In the end of the 3 weeks cultivation, the FW of the biomass was weighed again. 6 successful repetitions of the experiment were done between January and July 2017.

3.3. Temperature and irradiance

Data regarding ambient temperature and irradiance during the experiment period was extracted from the IMS data base from the Israel Meteorological Services (http://www.ims.gov.il/IMS/CLIMATE/LongTermRadiation/). Temperature (°C) data was based on the Tel Aviv coastal measurement station, which provides information in a 3 h resolution. Solar irradiance data (kW m^{-2}) was based on the Beit Dagan measurement station, which provides information about accumulated global irradiance with 1 h resolution. In the current work, hourly solar irradiance power per square meter was summed to produce daily solar irradiance energy per square meter (kWh m^{-2} day^{-1}). Fig. 3 presents how temperature and daily irradiance energy per square meter changed along the experiments period. Solar irradiance data was used to evaluate EE. Temperature data was used to examine temperature effects on biomass production.

3.4. Exergy analysis

Both EE and ExROI were calculated according to Eqs. (3) and (4), based on the experiment's results, system's structure and meteorological data from certified sources.

E_{sol} was calculated by Eq. (5):

$$E_{sol} = I\cdot W\cdot A \tag{5}$$

where I is the average daily solar irradiance for the cultivation period, W is a constant figure representing irradiance lost by the building's shading, and A is the sleeve area exposed to the sun. I, the average daily global solar irradiance (kWh m^{-2} day^{-1}), was calculated based on IMS data base from the Israel Meteorological Services from Beit Dagan Israel measurement station (See 3.3), W, the constant figure representing irradiance left after building's shading losses, was defined as 0.1, as described in the previous MPBR description [6]. A, the sleeve area exposed to the sun, as can be calculated from the dimensions shown in Fig. 1, is 0.18 m^2.

E_{elec} was measured as the power needed to run the air pump continuously during day time, while photosynthesis occurs, and for 15 min mixing pulses three times during night time, thus avoiding anoxic conditions, both at a rate of 2 L min^{-1}. E_{elec} was measured to be 0.008 kWh day^{-1}. This measurement does not consider previous energy losses due to conversion from primary energy sources into electricity.

E_{nut} was calculated based on the conversion of chemical fertilizers to energy, as presented by [51]. This conversion suggests that 1 kg of nitrogen (N) is equivalent to 66.14 MJ and 1 kg of phosphorus pentoxide (P_2O_5) is equivalent to 12.44 MJ. Using these conversions to calculate the exergetic equivalence of the added concentrations, yields a daily value of $5.5\cdot 10^{-4}$ kWh day^{-1} for the added nitrogen and $3.3\cdot 10^{-5}$ kWh day^{-1} for the added phosphorus.

E_{bio} was calculated by Eq. (6):

$$E_{bio} = EC\cdot DW{:}\ FW\cdot bio \tag{6}$$

where EC is the energy content that was determined as 9.879 MJ kg^{-1}, based on caloric value analysis done by a certified laboratory of Israel Electric company according to ASTM D5865-13 (Standard Test Method for Gross Calorific Value of Coal and Coke), as shown in [6]. DW: FW is the dry weight to fresh weight ratio, which was defined as 0.15, based on the previous work [6]. bio is the biomass FW divided by 21 for normalizing it per day. Exergy input and output streams are summarized in Table 1.

3.5. Sensitivity analysis

A sensitivity analysis was performed to examine the immediate

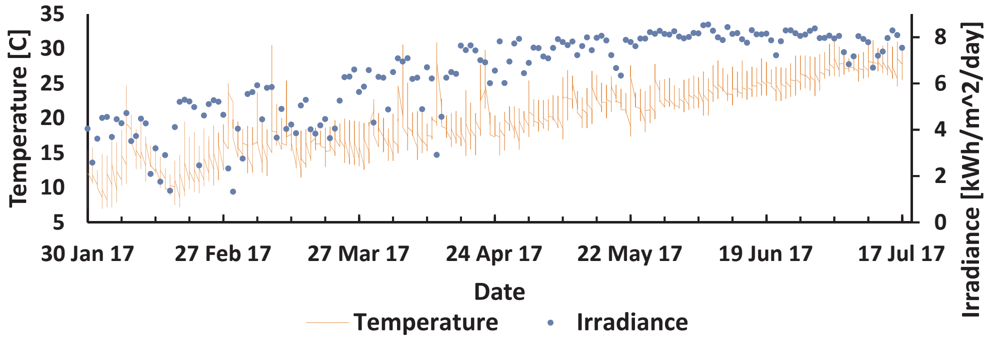

Fig. 3. Variation of temperature and daily solar irradiance energy per square meter with time along the experiments period.

potential increase in the energetic efficiency of the MPBR system. The focus of this analysis was on initial biomass density, although some other parameters, such as air flow rate and nutrient quantities can have significant effects too. A theoretical growth model was built to simulate the final biomass resulting from different initial densities. The model was based on results published by Nikolaisen and colleagues [16] regarding average growth rates of *Ulva Lactuca* in different densities in cultivation reactors. These results show that the mean absolute growth rate per horizontal area, presented in units of g DW m^{-2} day^{-1}, increases till a maximum of 38.8 at a density of 4 kg FW m^{-2} and then decreases. This decrease is explained by self-shading of the algae. The model (Fig. 4a and Eq. (8)) was built firstly by assuming a sigmoidal growth rate vs density curve [52–54]. Next, the growth was constrained to fit the measurements of the current study, namely a mean density growth of 0.2 kg FW m^{-2} to 1.4 kg FW m^{-2} within 21 days. Last, the squared difference between the previously measured mean growth rates [16] and the model results was minimized. This was done using the solver tool of Microsoft Excel (2016), as explained in [55], and is relevant for the first part of the curve, below the maximum. Above the maximum, a simple logarithmic trend line was fitted to the mean results of [16], built continuously to the first part (Fig. 4b).

Total Relative Error (TRE) of the first part of the model was calculated using Eq. (7), where m is the number of measurements, S_i is the measured value, and PV_i is the predicted value.

$$TRE = \frac{100}{m}\sqrt{\sum_{i=1}^{m}\left(\frac{S_i - PV_i}{PV_i}\right)^2} \quad (7)$$

The relative errors of the model for 1, 2 and 4 kg FW m^{-2} was 0.8%, 15.3% and 14.8%, respectively, and the TRE was 7.1%. The significant deviation between model and measured results in the densities of 2 and 4 kg FW m^{-2} result from the limitations of the theoretical sigmoidal model to describe mean growth rates of values measured along eight weeks in possibly varying ambient conditions. However, this model is useful for simulating how the performance parameters such as EE and ExROI can change with varying densities.

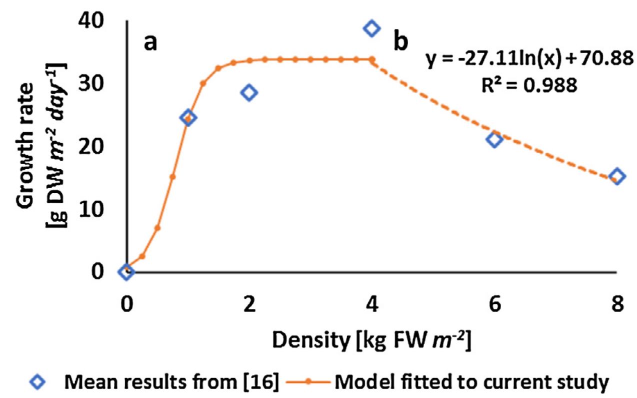

Fig. 4. Growth rate vs density model. (a) Below maximum, a sigmoidal curve built to best-fit results from [16] and from the current study. (b) Above maximum, a logarithmic decrease built continuously according to the results of [16].

Table 1
Exergy input and output streams summary.

	Description	Equation/value	Units	Reference
Input exergy streams				
E_{sol}	Average daily local solar irradiance energy	$E_{sol} = I{\cdot}W{\cdot}A$	kWh day^{-1}	Equation (5)
I	Average daily global solar irradiance	Varies	kWh m^{-2} day^{-1}	Israel Meteorological Services
W	Factor representing irradiance left after building's shading losses	0.1	[–]	[6]
A	Sleeve area exposed to the sun	0.18	m^2	Fig. 1
E_{elec}	Air pump electrical energy consumption	0.008	kWh day^{-1}	
$E_{bio\ initial}$	E_{bio} = *energy cont ·DW:FW ·bio*		kWh day^{-1}	Eq. (6)
energy cont	Energy content of biomass	9.879	MJ kg^{-1}	[6]
DW:FW	Dry weight to fresh weight ratio	0.15	[–]	[6]
bio	Initial biomass FW normalized per day	0.00048	kg day^{-1}	Current study's results
E_{nut}	Chemical fertilizers converted to energy		kWh day^{-1}	
	1 kg of nitrogen (N)	66.14	MJ kg^{-1}	[51]
	1 kg of phosphorus pentoxide (P2O5)	12.44	MJ kg^{-1}	[51]
Output exergy stream				
$E_{bio\ produced}$		E_{bio} = EC·*DW:FW ·bio*		Eq. (6)
EC	Energy content of biomass	9.879	MJ kg^{-1}	[6]
DW:FW	Dry weight to fresh weight ratio	0.15	[–]	[6]
bio	Produced biomass FW normalized per day	Varies	kg day^{-1}	Current study's results

Table 2
Measured energy streams and efficiencies in current study.

Return	Dates	Input exergy streams [kWh month^{-1}]				Output energy stream [kWh month^{-1}]	EE	ExROI
		Initial Biomass	Irradiance	Air blower	Nutrients	Produced Biomass		
1	30/1-20/2	0.006	2.129	0.233	0.018	0.029	0.012	0.139
2	20/2-13/3	0.006	2.433	0.233	0.018	0.020	0.008	0.105
3	30/4-21/5	0.006	3.954	0.233	0.018	0.037	0.010	0.173
4	22/5-12/6	0.006	4.258	0.233	0.018	0.046	0.010	0.208
5	5/6-26/6	0.006	4.258	0.233	0.018	0.049	0.011	0.218
6	26/6-17/7	0.006	4.258	0.233	0.018	0.029	0.006	0.140

$$Biomass\ [\text{g FW}] = \frac{81.3}{2.4 + 13.4 \cdot \exp(-4.6 \cdot (t\,[\text{days}] - 0.4)} \tag{8}$$

4. Results and discussion

4.1. MPBR energetic performance

Ulva was cultivated in the closed MPBR for 6 following periods of 21 days between January and July 2017. Table 2 presents the exergy input and output streams of each experiment, calculated by the procedures described in Section 3.4. As the system was not isolated from environmental factors such as solar irradiance and ambient temperature, that are presented in Section 3.3, the local climate affected the results. Irradiance had a direct effect, as it is a fundamental part of the photosynthesis process [56]. Temperature, although it is not presented in the photosynthesis formula, affects all physiological processes, including the algae growth rate [50,57,58] and therefore affected the results too.

Fig. 5 presents the contribution of the different input energy streams to EE and ExROI. In the EE, the major input exergy stream is the solar energy. In the ExROI, the major input exergy stream is the electrical energy.

Fig. 6 presents EE and ExROI variation with ambient conditions. With the exception of the last return, a monotonic and linear increase of ExROI with irradiance was identified (Spearman's r = 0.95, Pearson's r = 0.96, Fig. 6a). This linear increase of ExROI with irradiance corresponds with a monotonic and linear increase of the produced biomass with irradiance (Spearman's r = 0.95, Pearson's r = 0.95, Fig. 7), as the produced biomass is the only dependent variable in the ExROI formula. This correlation confirms that nutrients and CO_2 were supplied in excess and that the main limiting growth factor within this study was the irradiance. The last return did not follow the trend and therefore was not included in the identified trend line (Fig. 6a, red circle). This exception can be explained by the temperature (above 27 °C in average, Fig. 6b) which was probably beyond the optimum for this species and lead to a decreased growth. Previous works have shown that the photosynthetic efficiency of *Ulva Linza* declines above 25 °C in late-stage vegetation and above 15 °C in early-stage vegetation [58].

Unlike the ExROI, the EE was not affected by irradiance or temperature change, except for the decrease in the highest temperature. Examination of the EE components reveals that the irradiance is the dominant parameter in the denominator of the equation and the produced biomass is the only parameter in its numerator. Furthermore, the linear relation (Pearson's r = 0.84, Fig. 6c) that is found between the final biomass and the irradiance leads to an EE that does not variate with irradiance. These insights, of course, relate only to similar cultivation conditions and proportions between the different exergy input streams, and specifically to a suitable temperature range.

4.2. Exergetic efficiencies in algae cultivation systems

As the research in the macroalgae biomass field is not as developed as the research in the microalgae field, MPBR performances are compared to the performances of microalgae cultivation systems. Table 3 presents figures of exergy consumption and ExROI in our building integrated MPBR from the current work and in some building-integrated photobioreactors (PBRs) from the work done recently by Pruvost and colleagues [34], normalized to the production of 1000 kg DW biomass per year. The preoptimized ExROI of our MPBR, 0.14, lies around the middle of the 0.013–0.327 ExROI range of building-integrated microalgae PBRs, and seemingly above the median. Table 4 presents some more ExROI values, this time with different systems that are mostly of a bigger scale. The figures in this table show that algae cultivation systems with positive ExROI do exist, thus offering models to learn from. All ExROI values in this work, unless stated otherwise, relate only to cultivation exergy input streams and ignore other pre-cultivation or processing exergy inputs. These excluded exergy streams have a significant effect on the ExROI of large scale fuel production but are out of the scope of the current work. Further comparisons to other, non-algal, biological processes, should take into account also the "Cumulative Degree of Perfection" (CDP) term, which has the same mathematical expression as the ExROI [59], and is used by some researchers. For example, Huysveld and colleagues have compared resource efficiency

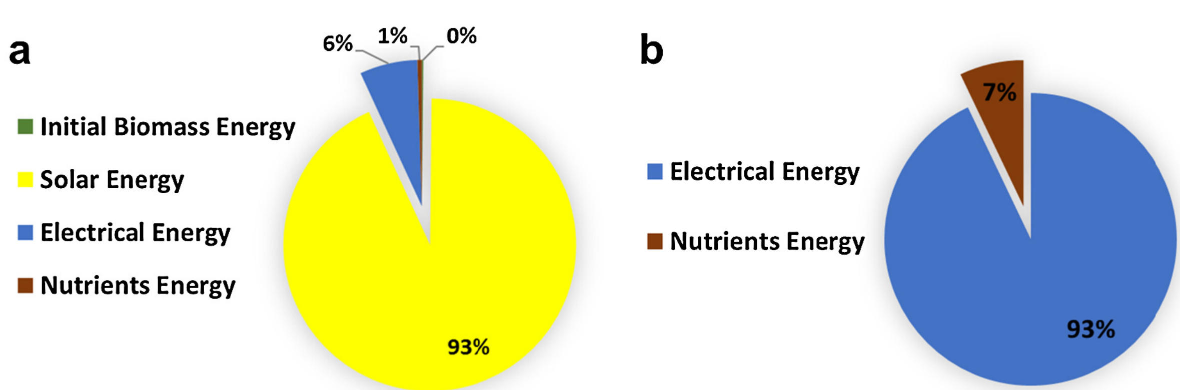

Fig. 5. Contribution of different input exergy streams to EE (a) and ExROI (b).

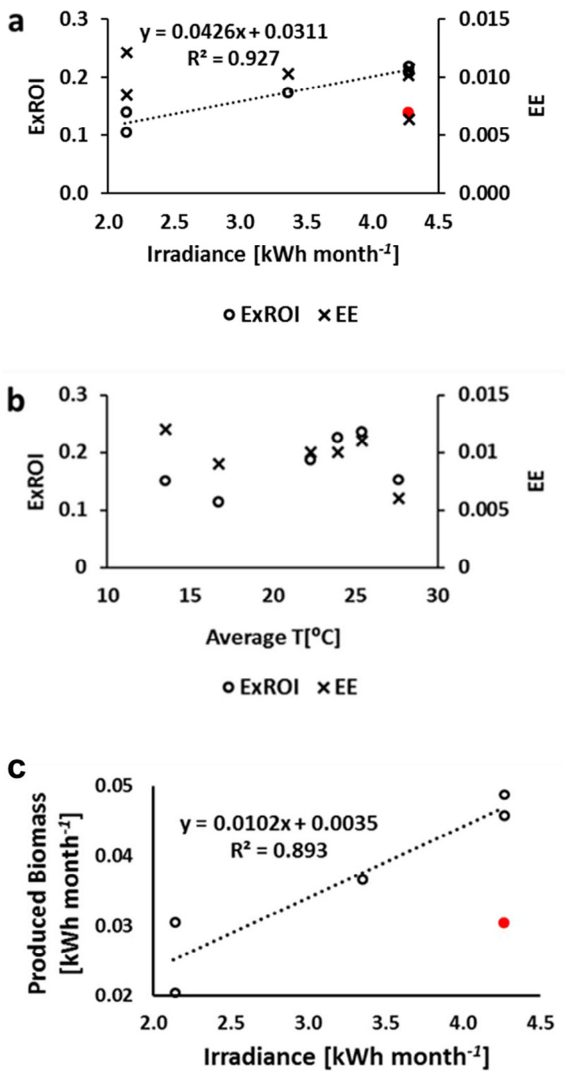

Fig. 6. *Ulva* EE and ExROI variation with measured ambient conditions within the current study. (a) Irradiance (red circle represents the last return, which did not follow the trend) (Pearson's r = 0.96) (b) Average T [°C]. (c) Produced *Ulva* biomass variation with irradiance. The red circle represents the last return, which did not follow the trend (Pearson's r = 0.87). Other exergy input streams remain constant.

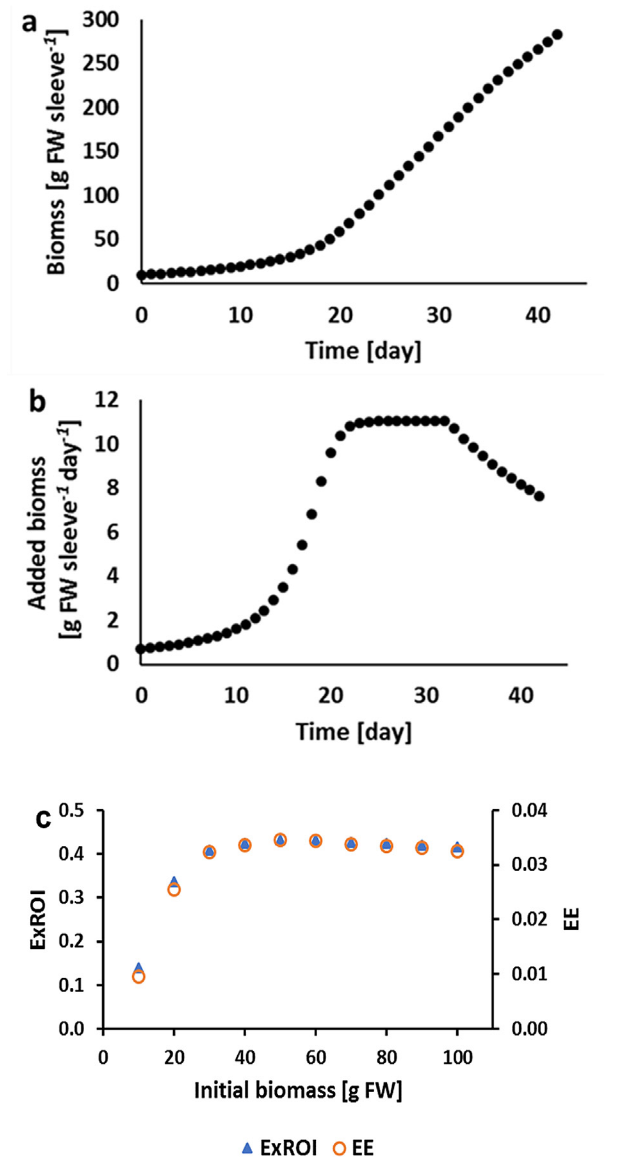

Fig. 7. The growth model of the algae in the sleeve. (a) Accumulated biomass with time. (b) Daily growth rate with time. (c) MPBR ExROI and EE projected change with initial biomass density.

of bio-based products and their fossil-derived counterparts using different CDP calculation methods [60]. Another example, is the work of Özilgena and Sorgüven, that assessed the CDP of soybean, olive and sunflower oil to be 0.92, 0.98 and 2.36, respectively, and suggested that olive and soybean CDP can be raised to 1.6 and sunflower oil CDP to 2.9 by good agricultural practices and substitution of diesel with biodiesel from renewable sources [61]. Final products such as bio-fuels, could be further assessed using the renewability indicator, which defines an energy source as renewable if the useful work gained by that source is larger than the work required to restore the environment to its initial state [62].

4.3. Areal and volumetric productivity in algae cultivation systems

At the same time, it should be mentioned that energetic efficiency is not the only evaluation parameter for energy harnessing systems. Since these systems can be integrated into buildings and dense urban environments, and since the biofuel – land agriculture conflict is one of the big challenges of the biofuel industry, evaluation of areal and volumetric footprints is also important. Table 5 presents the footprint figures of a few different systems. A comparison between the footprint figures of building-integrated systems, places the closed MPBR, relatively to existing microalgae systems, in a similar areal productivity scale (0.007 kg DW m^{-2} day^{-1} compared to 0.0078 and 0.098 kg DW m^{-2} day^{-1}) and very low in the volumetric productivity range (0.012 g DW l^{-1} day^{-1} compared to 0.15 and 0.18 g DW l^{-1} day^{-1}). Therefore, raising the algae density in the MPBR and thus the volumetric productivity, is one important direction for improvement.

4.4. Sensitivity analysis

The growth rate vs density model which is presented in the methods chapter (3.4), enabled the production of a biomass vs time curve (Fig. 7a), which was used for the calculation of the final biomass and thus enabled the prediction of EE and ExROI values. Fig. 7b models the daily accumulated biomass. Due to little data, the growth curves were not continued further. However, a decreasing trend of the growth rate is clear, and therefore the accumulated biomass is expected, in high

Table 3
Energy consumption and ExROI values for the production of 1000 kg DW biomass year^{-1} in building-integrated PBRs.

	Total energy consumption [kWh month^{-1}]	ExROI for biomass production	Reference	Note
Facade PBR without thermal symbiosis	35,000	0.013	[34]	[1]
Facade PBR with thermal symbiosis	5000	0.093	[34]	[1]
Facade PBR - reduced depth, no mixing at night, 50% thermal symbiosis	1417	0.327	[34]	[1]
PBR at optimal inclination (45), no thermal symbiosis	28,750	0.016	[34]	[1]
Raceway	12,500	0.037	[34]	[1,2]
MPBR	1508	0.140	Current study	

[1] Energy consumption in the energetic analysis based solely on the energy required for mixing and thermal regulation.
[2] Not a building-integrated system. Was added as a reference.

Table 4
ExROI values for the different algae production set ups.

	ExROI[4] for biomass production	Reference	Note
Raceway	8.34	[35]	[1]
Flat-plate photobioreactors	4.51	[35]	[1]
Tubular photobioreactors	0.20	[35]	[1]
Hybrid energy system	0.05–7.64	[36]	[2]
Off-shore macroalgae production	0.47–2.94	[33]	[3]
MPBR	0.140	Current study	

[1] Energy consumption in the energetic analysis based solely on the energy required for air pumping.
[2] Energy analysis is based on the cultivation stage. Energy required for preparation of culture, CO_2 injection, biomass separation and drying, oil extraction and biodiesel production are excluded from the analysis.
[3] Energy consumption in energetic analysis includes crop cultivation and also harvesting and processing into biofuel.
[4] Original papers used the terms EROI (Energy Return On Investment) or NER (Net Energy Ratio), but calculated it by the current study ExROI formula.

Table 5
Occupied areal and volumetric productivity values for the different algae production setups.

	Occupied areal productivity [kg DW m^{-2} day^{-1}]	Volumetric productivity [g DW l^{-1} day^{-1}]	Reference
Facade PBR - no thermal symbiosis	0.0078	0.15	[34]
PBR at optimal inclination (45), no thermal symbiosis	0.0098	0.18	[34]
Flat-plate photobioreactors	0.027	0.27	[34]
Tubular photobioreactors	0.025	0.56	[35]
Photobioreactors	N/A	0.4–1.9	[37]
Hybrid energy system	0.0179–0.0313	0.057–0.0997	[36]
Raceway ponds	0.0055	0.029	[34]
Raceway ponds	0.011	0.035, 0.07–0.18	[36,37]
MPBR	0.007	0.012	Current study

densities, to reach a saturation or even a negative growth.

Table 6 presents the growth results of 10 chosen initial densities and the consequent energy streams. Although the nutrients were used in excess, for this analysis extra nutrients were added according to the ratio between the projected biomass production and the original production. Irradiance was assumed to be the average of the measurements, 3.4 kWh month^{-1}.

As clearly visible in Fig. 7c, ExROI and EE increase with raising initial density till a saturation point. This efficiency saturation is achieved with initial densities of about 50 g FW per sleeve, or 1 kg FW per square meter, and yield an ExROI value of roughly 0.433. The saturation shape of the ExROI curve, followed by a slow decrease, is explained by the shading effect, being more significant in high densities. The similarity between the EE and the ExROI curves derives from the mathematical similarity of both equations (Eqs. (3) and (4)), reacting to changes in the produced biomass and in the added nutrients in a similar manner.

4.5. MPBR optimization

Fig. 8a and b presents the effect of the biomass density optimization, suggested above, on the MPBR performances, compared to the existing figures. Fig. 8a shows a comparison between ExROI values in building-integrated PBRs, including the projected ExROI value of density-optimized MPBR (dashed column). This projected ExROI, 0.433, that should be used cautiously, is significantly higher than values achieved in other building-integrated systems. However, even when taking this value into account, and similarly to most known photobioreactors [37], the exergy efficiency of the MPBR from the current study is still negative (less than 1), and therefore optimization and improvements are yet to be done.

Fig. 8b shows a comparison between footprint figures in building-integrated PBRs, including the projected values of density-optimized MPBR (dashed columns). According to this analysis, areal and volumetric productivities of the MPBR can be improved to 0.025 kg DW m^{-2} day^{-1}, and 0.044 g DW l^{-1} day^{-1}. These numbers set this system close to the top of the known areal productivities but still quite low in the volumetric productivity.

Finally, on top of the obvious necessity of implementing the biomass density optimization, these results reflect also the importance of research regarding efficient nutrient usage and air flow mixing, which are essential for further optimization of MPBR systems towards positive ExROI values. Furthermore, future work should also analyze the economics of macroalgae cultivation, an analysis that would not be effective in the current scale.

5. Conclusions

The current work presents detailed procedures for the measurement of two exergetic efficiency indicators, adjusted specifically to macroalgae laboratory scale cultivation systems. Based on growth measurements of Ulva sp. cultivated in a MPBR incorporated into building for 6 following 21 days periods, first exergy efficiency values are suggested herein. The limitations of this analysis relate to the inability to reliably compare all the systems according to ExROI values only. Thus, for instance, our density optimized system yields an ExROI of 0.433 and area usage of 0.025 kg DW m^{-2} day^{-1} while the highest ExROI type is raceway (8.34) that has an inherent problem of area usage (only 0.0055 kg DW m^{-2} day^{-1}). These projected exergetic efficiencies are still low, and further improvement will be achieved based on optimization of nutrient addition and mixing methodology. Finally, this work offers evaluation tools and preliminary results useful for future research and development in macroalgae cultivation studies.

Table 6
Exergy input and output streams assuming different initial biomass densities.

Biomass [g FW]		Density [kg FW m^{-2}]		Energy streams [kWh $month^{-1}$]				
Initial	Final	Initial	Final	Air blower	Nutrients	Produced biomass	EE	ExROI
10	69	0.2	1.4	0.233	0.018	0.035	0.010	0.140
20	178*	0.4	3.6	0.233	0.048**	0.094	0.026	0.336
30	231*	0.6	4.7	0.233	0.061**	0.120	0.032	0.409
40	250*	0.8	5.1	0.233	0.063**	0.125	0.034	0.423
50	266*	1.0	5.4	0.233	0.065**	0.129	0.035	0.433
60	275*	1.2	5.6	0.233	0.065**	0.128	0.034	0.431
70	282*	1.4	5.7	0.233	0.064**	0.126	0.034	0.426
80	290*	1.6	5.9	0.233	0.063**	0.125	0.033	0.423
90	298*	1.8	6.1	0.233	0.063**	0.124	0.033	0.420
100	305*	2.0	6.2	0.233	0.062**	0.122	0.033	0.415

* Projected based on growth model (Fig. 7).
** Nutrients were added according to the ratio between the projected biomass production and the original production.

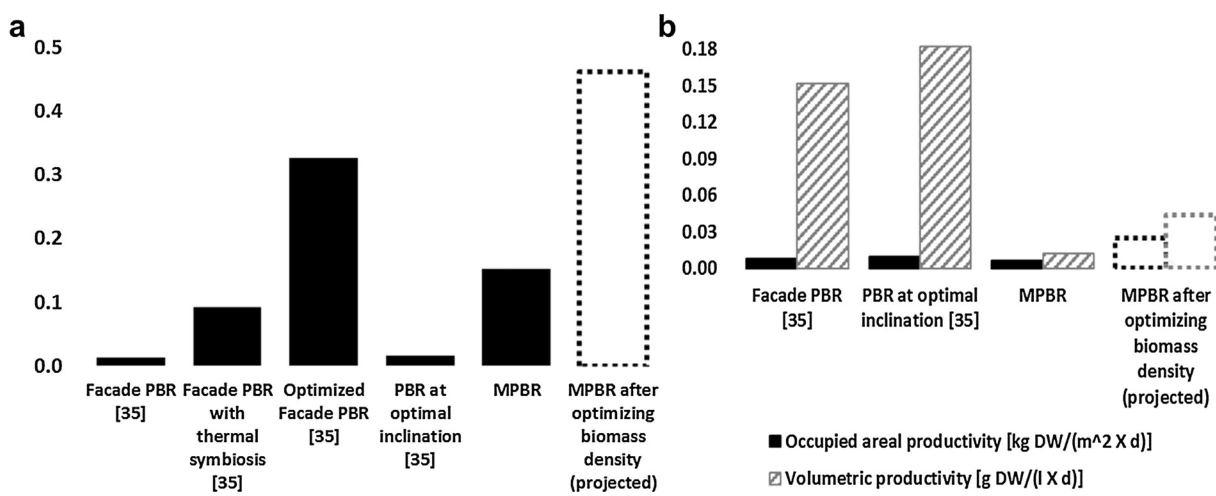

Fig. 8. (a) A comparison between ExROI values in building-integrated PBRs. In contrast to the macroalgae MPBR, literature values [34] relate to microalgae cultivation systems. (b) A comparison between areal and volumetric footprints in building-integrated PBRs. In contrast to the macroalgae MPBR, literature values [34] relate to microalgae cultivation systems.

Acknowledgments

The authors thank TAU Institute for Innovation in Transportation, TAU Gordon Center for Energy, Israel Ministry of Energy and Israel Ministry of Science and Technology for funding.

Competing interest statement

The authors declare no conflict of interest.

References

[1] Ptasinski KJ. Efficiency of biomass energy: an exergy approach to biofuels, power, and biorefineries. John Wiley & Sons; 2016.
[2] Bilgen S. Structure and environmental impact of global energy consumption. Renew Sustain Energy Rev 2014;38(Oct.):890–902.
[3] Strzalka U, Schneider R, Eicker D. Current status of bioenergy technologies in Germany. Renew Sustain Energy Rev 2017:801–20.
[4] Kraan S. Mass-cultivation of carbohydrate rich macroalgae, a possible solution for sustainable biofuel production. Mitig Adapt Strateg Glob Chang 2013;18(1):27–46.
[5] Fernand F, Israel A, Skjermo J, Wichard T, Timmermans KR, Golberg A. Offshore macroalgae biomass for bioenergy production: environmental aspects, technological achievements and challenges; 2017.
[6] Chemodanov A, Robin A, Golberg A. Design of marine macroalgae photobioreactor integrated into building to support seagriculture for biorefinery and bioeconomy. Bioresour Technol 2017;241:1084–93.
[7] Golberg A, Vitkin E, Linshiz G, Khan SA, Hillson NJ, Yakhini Z, et al. Proposed design of distributed macroalgal biorefineries: thermodynamics, bioconversion technology, and sustainability implications for developing economies. Biofuels Bioprod Biorefining 2014;8(1):67–82.
[8] Lehahn Y, Ingle KN, Golberg A, Nivrutti K, Golberg A. Global potential of offshore and shallow waters macroalgal biorefineries to provide for food, chemicals and energy: feasibility and sustainability. Algal Res 2016;17:150–60.
[9] Ringler C, Bhaduri A, Lawford R. The nexus across water, energy, land and food (WELF): potential for improved resource use efficiency? Curr Opin Environ Sustain 2013;5(6):617–24.
[10] Bharathiraja B, Chakravarthy M, Ranjith Kumar R, Yogendran D, Yuvaraj D, Jayamuthunagai J, et al. Aquatic biomass (algae) as a future feed stock for bio-refineries: a review on cultivation, processing and products. Renew Sustain Energy Rev 2015;47:634–53.
[11] Hafting JT, Craigie JS, Stengel DB, Loureiro RR, Buschmann AH, Yarish C, et al. Prospects and challenges for industrial production of seaweed bioactives. J Phycol 2015;51(5):821–37.
[12] Neori A, Msuya FE, Shauli L, Schuenhoff A, Kopel F, Shpigel M. A novel three-stage seaweed (Ulva lactuca) biofilter design for integrated mariculture. J Appl Phycol 2003;15(6):543–53.
[13] Neori A, Cohen I, Gordin H. Ulva lactuca biofilters for marine fishpond effluents. II. Growth rate, yield and C:N ratio. Bot Mar 1991;34(6):483–90.
[14] van den Burg S, Stuiver M, Veenstra F, Bikker P, López Contreras A, Palstra A, et al. A triple P review of the feasibility of sustainable offshore seaweed production in the North Sea; 2013.
[15] Bruhn A, Dahl J, Nielsen HB, Nikolaisen L, Rasmussen MB, Markager S, et al. Bioenergy potential of Ulva lactuca: biomass yield, methane production and combustion. Bioresour Technol 2011;102(3):2595–604.
[16] Nikolaisen L, Jensen PD, Bech KS. Energy production from marine biomass (Ulva lactuca); 2008. p. 1–72.
[17] Saqib A, Tabbssum MR, Rashid U, Ibrahim M, Gill SS, Mehmood MA. Marine macro algae ulva: a potential feed-stock for bio- ethanol and biogas production. Asian J Agri Biol 2013;1(3):155–63.
[18] Balina K, Romagnoli F, Pastare L, Blumberga D. Use of macroalgae for bioenergy production in Latvia: review on potential availability of marine coastline species. Energy Procedia 2017;113(May):403–10.
[19] Park SK, Pandey SR, Tyagi AK, Tyagi VV. Energy and exergy analysis of typical renewable energy systems. Renew Sustain Energy Rev 2014:105–23.

[20] Arvidsson R, Fransson K, Fröling M, Svanström M, Molander S. Energy use indicators in energy and life cycle assessments of biofuels: review and recommendations. J Clean Prod 2012;31:54–61.
[21] Lee W, Den M. Life cycle value analysis for sustainability evaluation of bioenergy products. J Clean Prod 2016:541–7.
[22] Boschiero S, Cherubini M, Nati F, Zerbe C. Life cycle assessment of bioenergy production from orchards woody residues in Northern Italy. J Clean Prod 2016:2569–80.
[23] Jungbluth J, Chudacoff N, Dauriat M, Dinkel A, Doka F, Emmenegger G, et al. Life cycle inventories of bioenergy. Final report ecoinvent data v2. 0 No. 17, technical report. Dϋbendorf, CH; 2007.
[24] Dresselhaus MS, Thomas IL. Alternative energy technologies. Nature 2001;414(6861):332–7.
[25] Kamran Taheri AK, Gadowa Rainer. Exergy analysis as a developed concept of energy efficiency optimized processes: the case of thermal spray processes. Procedia 2014.
[26] Kanoglu MRM, Dincer I. Understanding energy and exergy efficiencies for improved energy management in power plants. Energy Policy 2007.
[27] Nikulshin VNV, Wu C. Exergy efficiency calculation of energy intensive systems. Exergy Int J 2002.
[28] Rosen MA, Bulucea CA. Using exergy to understand and improve the efficiency of electrical power technologies. Entropy 2009;11(4):820–35.
[29] Exergy life cycle assessment of a waste-to-energy plant. Energy Procedia 2016;104(Dec.):562–7.
[30] Assessment of biodiesel energy sustainability using the exergy return on investment concept. Energy 2012;45(1):474–80.
[31] Raman V, Tiwari GN. A comparison study of energy and exergy performance of a hybrid photovoltaic double-pass and single-pass air collector. Int J Energy Res 2009;33(6):605–17.
[32] Bakshi DP, Gutowski BR, Sekulic TG. Thermodynamics and the destruction of resources. Cambridge University Press; 2011.
[33] Carneiro MLNM, Pradelle F, Braga SL, Gomes MSP, Martins ARFA, Turkovics F, et al. ethanol and biodiesel in Europe and Brazil through life cycle assessment (LCA). Renew Sustain Energy Rev 2017;73(April):632–53.
[34] Pruvost J, Le Gouic B, Lepine O, Legrand J, Le Borgne F. Microalgae culture in building-integrated photobioreactors: biomass production modelling and energetic analysis. Chem Eng J 2016;284:850–61.
[35] Jorquera O, Kiperstok A, Sales EA, Embiruçu M, Ghirardi ML. Comparative energy life-cycle analyses of microalgal biomass production in open ponds and photobioreactors. Bioresour Technol 2010;101(4):1406–13.
[36] Shahnazari M, Bahri PA, Parlevliet D, Minakshi M, Moheimani NR. Sustainable conversion of light to algal biomass and electricity: a net energy return analysis. Energy 2017;131:218–29.
[37] Hallenbeck PC, Grogger M, Mraz M, Veverka D. Solar biofuels production with microalgae. Appl Energy 2016;179:136–45.
[38] Raja R, Hemaiswarya S, Kumar NA, Sridhar S, Rengasamy R. A perspective on the biotechnological potential of microalgae. Crit Rev Microbiol 2008;34(2):77–88.
[39] Slade R, Bauen A. Micro-algae cultivation for biofuels: cost, energy balance, environmental impacts and future prospects. In: 20th Eur biomass conf, vol. 53, no. 0; 2013. p. 29–38.
[40] Jonker JGG, Faaij APC. Techno-economic assessment of micro-algae as feedstock for renewable bio-energy production. Appl Energy 2013;102:461–75.
[41] Microalgae-based biodiesel: economic analysis of downstream process realistic scenarios. Bioresour Technol 2013;136(May):617–25.
[42] Whiting K, Carmona L, Carrasco A, Sousa T. Exergy replacement cost of fossil fuels: closing the carbon cycle. Energies 2017;10(7):979.
[43] Exergy-based optimization of direct conversion of microalgae biomass to biodiesel. J Clean Prod 2017;141(Jan.):50–5.
[44] Yan Y, Muñoz C, Zhu R, Wang L. The effects of various LED (light emitting diode) lighting strategies on simultaneous biogas upgrading and biogas slurry nutrient reduction by using of microalgae Chlorella sp. Energy 2016:554–61.
[45] Atta S, Idris M, Bukhari A, Wahidin A. Intensity of blue LED light: a potential stimulus for biomass and lipid content in fresh water microalgae Chlorella vulgaris. Bioresour Technol 2013:373–8.
[46] Teo A, Atta CL, Bukhari M, Taisir A, Yusuf M, Idris AM. Enhancing growth and lipid production of marine microalgae for biodiesel production via the use of different LED wavelengths. Bioresour Technol 2014:38–44.
[47] Golberg A. Environmental exergonomics for sustainable design and analysis of energy systems. Energy 2015;88:314–21.
[48] Harrison CL, Hurd PJ. Nutrient physiology of seaweeds: application of concepts to aquaculture. Cah Biol Mar 2001:1–2.
[49] Parker HS. Influence of relative water motion on the growth, ammonium uptake and carbon and nitrogen composition of Ulva lactuca (Chlorophyta). Mar Biol 1981;63(3):309–18.
[50] Steffensen DA. The effect of nutrient enrichment and temperature on the growth in culture of Ulva lactuca L. Aquatic Botany 1976:337–51.
[51] Li H, Zhang Y, Han X, Shi X, Rivkin RB, Legendre L. Growth responses of Ulva prolifera to inorganic and organic nutrients: implications for macroalgal blooms in the southern Yellow Sea, China. Sci Rep 2016;6(1):26498.
[52] A proposed family of Unified models for sigmoidal growth. Ecol Modell 2017;359(Sep.);117–27.
[53] Hipkins R, Cowie B. The sigmoid curve as a metaphor for growth and change. Teach Curric 2016;16(2).
[54] Capture the time when plants reach their maximum body size by using the beta sigmoid growth equation. Ecol Modell 2016;320(Jan.):177–81.
[55] Kochmann S. Howto: fit sigmoid functions in OpenOffice Calc and Excel. THE WINNOWER – ISSN 2373-146X; 2017. [Online]. Available: https://thewinnower.com/papers/275-howto-fit-sigmoid-functions-in-openoffice-calc-and-excel [accessed: 01-Sep-2017].
[56] Ort DR, Yocum CF, Heichel IF. Oxygenic photosynthesis: the light reactions. Kluwer; 1996.
[57] Lehahn Y, Ingle KN, Golberg A. Global potential of offshore and shallow waters macroalgal biorefineries to provide for food, chemicals and energy: feasibility and sustainability; 2016.
[58] Kim JH, Kang EJ, Park MG, Lee BG, Kim KY. Effects of temperature and irradiance on photosynthesis and growth of a green-tide-forming species (Ulva Linza) in the Yellow Sea. J Appl Phycol 2011;23(3):421–32.
[59] Szargut J, Morris DR. Cumulative exergy consumption and cumulative degree of perfection of chemical processes. Int J Energy Res 1987;11(2):245–61.
[60] Huysveld S, De Meester S, Van linden V, Muylle H, Peiren N, Lauwers L, et al. Cumulative overall resource efficiency assessment (COREA) for comparing bio-based products with their fossil-derived counterparts. Resour Conserv Recycl 2015;102(Sep.):113–27.
[61] Özilgen M, Sorgüven E. Energy and exergy utilization, and carbon dioxide emission in vegetable oil production. Energy 2011;36(10):5954–67.
[62] Sorguven E, Özilgen M. Thermodynamic assessment of algal biodiesel utilization. Renew Energy 2010;35(9):1956–66.